Compatibilization Effect of Graft Copolymer on Immiscible Polymer Blends. II. LLDPE/PS/LLDPE-g-PS Systems

HANQIAO FENG,[1,*] JUN TIAN,[2] and CHAOHUI YE[1]

[1]Laboratory of Magnetic Resonance and Atomic and Molecular Physics, Wuhan Institute of Physics, The Chinese Academy of Sciences, Wuhan 430071, and [2]Polymer Physics Laboratory, Changchun Institute of Applied Chemistry, The Chinese Academy of Sciences, Changchun 130022, People's Republic of China

SYNOPSIS

The compatibilizing effect of graft copolymer, linear low density polyethylene-*g*-polystyrene (LLDPE-g-PS), on immiscible LLDPE/PS blends has been studied by means of ^{13}C CP-MAS NMR and DSC techniques. The results indicate that LLDPE-*g*-PS is an effective compatibilizer for LLDPE/PS blends, and the compatibilizing effect of LLDPE-*g*-PS on LLDPE/PS blends depends on the PS grafting yield and molecular structure of the compatibilizers and also on the composition of the blends. It was found that LLDPE-*g*-PS chains connect two immiscible components, LLDPE and PS, through solubilization of chemically identical segments of LLDPE-*g*-PS into the noncrystalline region of the LLDPE and PS domain, respectively. Meanwhile, LLDPE-*g*-PS chains connect the crystalline region of LLDPE by isomorphism, resulting in an obvious change in the crystallization behavior of LLDPE. © 1996 John Wiley & Sons, Inc.

INTRODUCTION

Recently, much attention has been paid to the study of using graft or block copolymers as compatibilizers for immiscible polymer blends because they are one of the simplest and most efficient means for development of new high-performance polymer materials.[1-10] Usually, suitably chosen graft or block copolymers, whose segment may be chemically identical with those in the respective phases or miscible with one of the phases, can act as "interfacial agents" to reduce interfacial tension and improve interfacial adhesion of the immiscible components. However, as pointed out in our previous article,[11] compatibilizers just located at the interfacial region may have quite different compatibilizing effects as compared with those connected two immiscible components by different chains. The former may have characteristic similar to low molecular weight emulsifiers, decreasing the interfacial tension and reducing phase growth by a steric stabilization mechanism. The latter can not only reduce the interfacial tension and enhance phase stability, but can also improve interfacial adhesion of the immiscible components by the bridge effects of the compatibilizer chains. As is well known, interfacial adhesion is a key factor affecting physical properties of multicomponent polymer materials with microphase separation, and hence their practical utility. The existence mode of compatibilizers in immiscible blends is the essence affecting their compatibilizing effects. Therefore, it is a prerequisite to exploring the compatibilization mechanism to detect the existence mode of compatibilizers in blends. As far as we know, much attention has been paid to the macroscopic effects of compatibilizers on morphology, interfacial properties, and mechanical behavior of immiscible polymer blends. It has been assumed that compatibilizers usually locate at the interfacial region between two immiscible components. However, only a few workers[8,10] obtained direct experimental evidence by electron microscopy, which supported the preceding assumption. Even so, the evidence could not tell whether or not the compatibilizers connected two immiscible components by the bridge effects of compatibilizer' chains. Hence, the real existence mode of compatibilizers in polymer blends

* To whom correspondence should be addressed.

Journal of Applied Polymer Science, Vol. 61, 2265–2271 (1996)
 CCC 0021-8995/96/132265-07

remains unknown due to the absence of suitable detecting techniques.

It is well known that (NMR) techniques can provide information about miscibility, molecular motion, and heterogeneity (morphology) of blends on a molecular level. In this work, the compatibilization effects of linear low density polyethylene-*g*-polystyrene (LLDPE-*g*-PS) with different PS grafting yield on immiscible blends of linear low density polyethylene (LLDPE) and polystyrene (PS) have been investigated by NMR and differential scanning calorimetry (DSC) techniques in order to explore the compatibilizing mechanism of LLDPE-*g*-PS on immiscible LLDPE/PS blends on a molecular level.

EXPERIMENTAL

Graft copolymers with different PS grafting yields, LLDPE-*g*-PS, were synthesized in our laboratory. The characterization data of the copolymers are listed in Table I.

PS ($M_w = 1.5 \times 10^5$, $T_g = 372$ K) and LLDPE ($M_w = 1.0 \times 10^5$, $T_m = 395.8$ K) were obtained from Yanshan Petro-Chemical Co. and Daqing Petro-Chemical Co., respectively. Both polymers were purified before use. Solution blending was used in this study, using toluene as a solvent and a solution concentration of 5% (w/v). The blends with different compositions, dissolved in the boiling toluene, were precipitated by pouring the solution into ethanol. After filtering, the products were washed with ethanol for several times. The blends were dried at room temperature and then dried under vacuum to a constant weight. All the blends were annealed under vacuum at 430 K for 5 h before being used for NMR and DSC experiments.

Solid-state ^{13}C CP-MAS NMR experiments were performed on a Bruker MSL-400 NMR spectrometer at 298 K. The total sideband suppression (TOSS) method was used for suppressing spinning side bands. The carbon-13 resonance frequency was 100.63 MHz, and the proton resonance frequency was 400.13 MHz. The dipolar decoupling field was about 49 kHz. ^{13}C spectra were referred to the shifts of methyl group carbons of hexamethylbenzene, which were 16.9 ppm.

DSC experiments were done using a Perkin-Elmer apparatus DSC-2 at a heating rate of 10 K/min.

RESULTS AND DISCUSSION

Usually, there are two peaks (32.2 ppm and 30.0 ppm)[11] in the ^{13}C CP-MAS spectrum of LLDPE.

Table I Characterization Data of Grafting Copolymers LLDPE-*g*-PS

No.	PS Grafting Yield in LLDPE-*g*-PS (wt %)	$M_w \times 10^{-4}$	Designation
1	2.0	8.09	GPS2
2	2.9	1.26	GPS3
3	3.6	0.87	GPS4
4	13.0	2.56	GPS13
5	17.0	—	GPS17
6	16.8	2.80	HGPS17*
7	27.0	4.88	GPS27

* Ethylene/PS–allyl copolymer.

The peak at 32.2 ppm was assigned to LLDPE chains in the crystalline region, and the peak at 30.0 ppm to LLDPE chains in the noncrystalline region.[12] Figures 1 and 2 show the typical plots of logarithmic intensity of ^{13}C CP-MAS spectra (peak at 32.2 ppm) of LLDPE and its blends with PS versus proton-spin-locking times. The corresponding proton spin-lattice relaxation times in the rotating frame, $T_{1\rho}(H)$, are listed in Table II. Here we can only detect the $T_{1\rho}(H)$ values of LLDPE chains in the crystalline region because the $T_{1\rho}(H)$ values of LLDPE chains in the noncrystalline region are too small to be measured at the same time. From Figures 1 and 2, and Table II, it is clearly seen that (1) there are two $T_{1\rho}(H)$ values for the crystalline peak of pure LLDPE and its blends; and (2) the addition of LLDPE-*g*-PS into LLDPE/PS blends gives rise to effects on the two $T_{1\rho}(H)$ values to different degrees. As is well known, a single $T_{1\rho}(H)$ value has been used as a criterion for the miscibility or homogeneity of multicomponent polymer systems.[13] The existence of two $T_{1\rho}(H)$ values in the crystalline region of LLDPE suggests that there exist heterogeneous domains in the crystalline region of LLDPE. A reasonable explanation for the existence of heterogeneity in the crystalline region is that coexistence of the perfect crystalline region and the less perfect crystalline region occurs in the crystalline region of LLDPE. Generally, the species in the relatively mobile region will have a shorter $T_{1\rho}(H)$ and a longer proton spin–spin relaxation time, $T_2(H)$. Hence, the chains with longer $T_{1\rho}(H)$ can be assigned to the perfect crystalline region, and the chains with shorter $T_{1\rho}(H)$ to the less perfect crystalline region. It was found that the effect of LLDPE-*g*-PS added to the two $T_{1\rho}(H)$ values of the crystalline region obviously depends on the composition of the LLDPE/PS blends. The addition

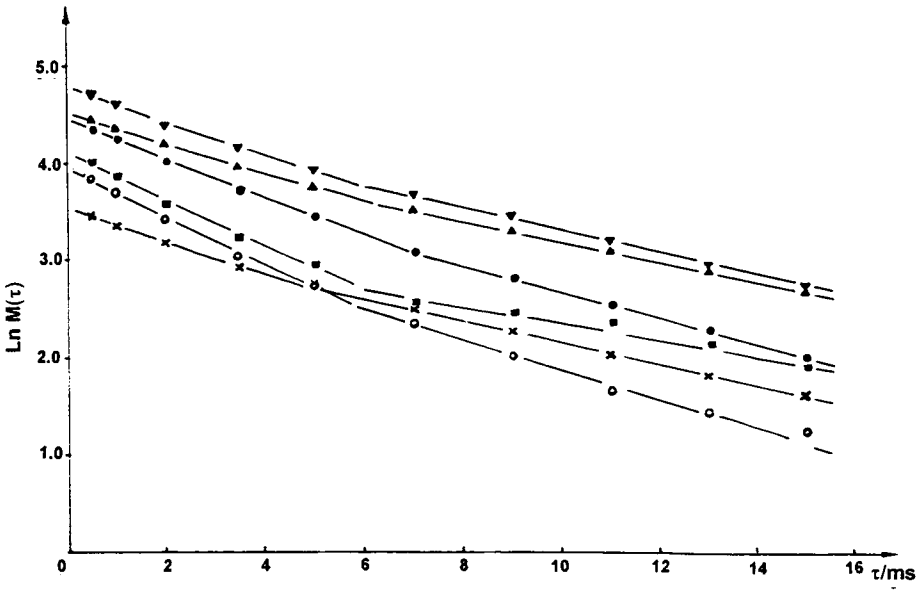

Figure 1 Plots of logarithmic intensity of the ^{13}C CP-MAS spectrum (peak at 32.2 ppm) of LLDPE and its blends versus proton-spin-locking time for (×) LLDPE, (○) LLDPE/PS, (●) LLDPE/PS-GPS4, (▼) LLDPE/PS-GPS13, (▲) LLDPE/PS-GPS17, and (■) LLDPE/PS-GPS27. The composition of LLDPE/PS-LLDPE-*g*-PS is 64/28/8 by weight.

of LLDPE-*g*-PS into LLDPE/PS (70/30) blends makes the longer $T_{1\rho}(H)$ become even longer and the shorter one almost remain unchanged. However, both the longer and the shorter $T_{1\rho}(H)$ values of LLDPE/PS (30/70) blends decrease due to the addition of LLDPE-*g*-PS. It was found that the ^{13}C spin-lattice relaxation time, $T_1(C)$, and $T_{1\rho}(H)$ values of semicrystalline polymers increase with their lamellar thickness.[14,15] Hence, the change of $T_{1\rho}(H)$ values of the crystalline region of LLDPE indicates that the lamellar thickness of LLDPE decreases or increases, depending on the PS grafting yield of LLDPE-*g*-PS added and the composition of LLDPE/PS blends. This conclusion is further supported by the results from DSC measurements of the same specimens.

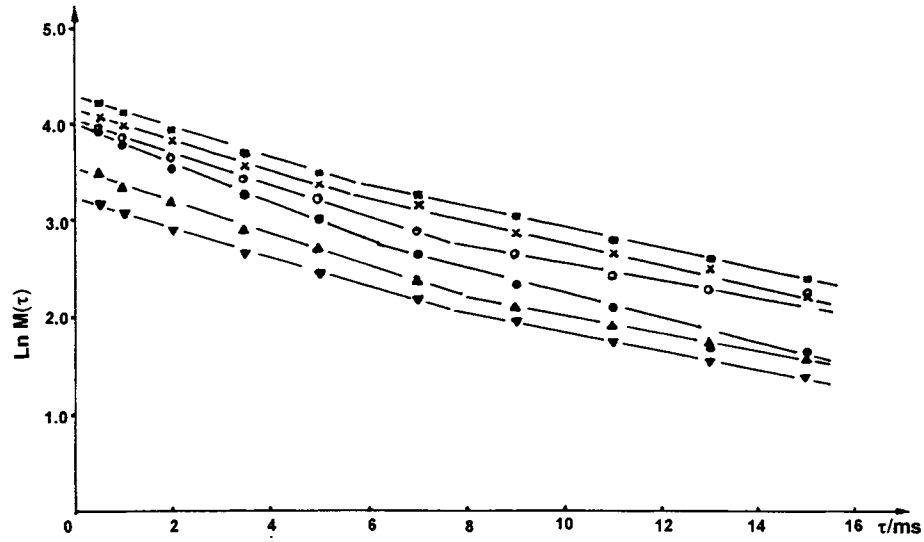

Figure 2 Plots of logarithmic intensity of the ^{13}C CP-MAS spectrum (peak at 32.2 ppm) of LLDPE and its blends versus proton-spin-locking time for (■) LLDPE, (×) LLDPE/PS, (○) LLDPE/PS-GPS4, (●) LLDPE/PS-GPS13, (▲) LLDPE/PS-GPS17, and (▼) LLDPE/PS-GPS27. The composition of LLDPE/PS-LLDPE-*g*-PS is 28/64/8 by weight.

Figure 3 shows the typical DSC traces of LLDPE/PS (30/70) blends with or without LLDPE-*g*-PS of different PS grafting yield. The corresponding melting point (T_m) and normalized heat of fusion (ΔH_f) are listed in Table III. There are two points worthy to be mentioned about Figure 3: (1) The addition of LLDPE-*g*-PS into LLDPE/PS (30/70) blends makes the melting point of LLDPE decrease; and (2) a new melting peak appears due to the addition of LLDPE-*g*-PS. It is well known that the melting point of polymer crystallite is mainly determined by its lamellar thickness.[16] Therefore, the depression of melting point of LLDPE in the LLDPE/PS (30/70) blends indicates the decrease in the lamellar thickness of LLDPE. The appearance of a new peak with a lower melting point suggests that some much less perfect crystallites form due to the addition of LLDPE-*g*-PS. Obviously, these results are in good agreement with those from NMR.

The addition of LLDPE-*g*-PS into PS blends not only affects the crystallization behavior of LLDPE, but also gives rise to a marked change in the morphology of the noncrystalline region of LLDPE. As mentioned earlier, the species in the relatively mobile region usually have a longer $T_2(H)$. Table IV shows the change of $T_2(H)$ values of LLDPE chains in the noncrystalline region with the content of LLDPE-*g*-PS added. It is found that (1) there are two $T_2(H)$ values in the noncrystalline region of LLDPE [the chains with longer $T_2(H)$ can be assigned to the amorphous or liquidlike region, and those with shorter $T_2(H)$ to the interfacial region between the crystalline region and noncrystalline region of LLDPE; and (2) both of the two $T_2(H)$ increase with the content of LLDPE-*g*-PS added. Meanwhile, the relative content of the shorter $T_2(H)$ component also increases with the content of LLDPE-*g*-PS. The increase in the $T_2(H)$ of the noncrystalline region suggests that the molecular motion in this region becomes even faster, and the enhancement in the relative content of shorter $T_2(H)$ indicates that the interfacial region of LLDPE is enlarged by the addition of LLDPE-*g*-PS. Obviously, the effect of LLDPE-*g*-PS on the morphological structure of LLDPE is related to the content of LLDPE-*g*-PS added. A marked change on the morphological structure of LLDPE can be detected when the content of LLDPE-*g*-PS added is about 2 wt %. Moreover, it is found that the effect of LLDPE-*g*-PS on the noncrystalline region is much larger than that on the crystalline region of LLDPE, implying that most of LLDPE-*g*-PS chains

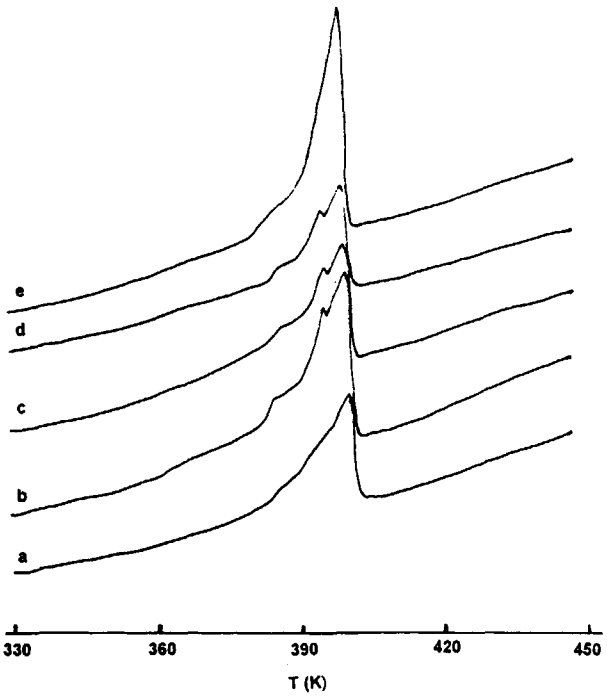

Figure 3 DSC traces of LLDPE/PS-LLDPE-*g*-PS (28/64/8) blends for (a) LLDPE–PS, (b) LLDPE/PS–GPS4, (c) LLDPE/PS–GPS13, (d) LLDPE/PS–GPS27, and (e) LLDPE/PS–HGPS17.

Table II Effect of PS Grafting Yield in LLDPE-*g*-PS on $T_{1\rho}(H)$ (ms)[a] of LLDPE/PS Blends

	LLDPE/PS (64/28) (32.2 ppm)				LLDPE/PS (28/64) (32.2 ppm)			
LLDPE-*g*-PS[b]	$T_{1\rho}(H)$	%	$T_{1\rho}(H)$	%	$T_{1\rho}(H)$	%	$T_{1\rho}(H)$	%
—	6.9	45.3	2.1	54.7	12.8	41.3	4.0	58.7
GPS4	7.5	60.9	2.2	39.1	9.9	57.3	3.1	42.7
GPS13	9.8	61.9	2.1	38.1	8.1	53.2	2.7	46.8
HGPS17	9.0	73.1	1.8	26.9	11.0	48.3	3.0	51.7
GPS27	16.9	25.9	2.5	74.1	11.2	57.0	2.8	30.0

[a] Estimated error $\leq \pm 5\%$.
[b] The content of LLDPE-*g*-PS in the blends is 8% by weight.

Table III Effect of PS Grafting Yield in LLDPE-*g*-PS on Melting Point (T_m), Normalized Heat of Fusion (ΔH_f), and Melting Range (T_{mr}) of LLDPE in LLDPE/PS Blends

LLDPE-*g*-PS[a]	LLDPE/PS (28/64) T_m (K)	ΔH_f (K)	T_{mr} (K)
—	397.3	68.0	367.4–404.5
GPS4	396.1, 391.7	73.0	343.8–402.3
GPS13	396.3, 391.6	77.2	343.1–401.9
HGPS17	396.9	96.7	352.8–403.3
GPS27	395.9, 390.4	68.9	340.0–403.8

[a] The content of LLDPE-*g*-PS in the blends is 8% by weight.

locate on the noncrystalline region of LLDPE. Therefore, we can conclude that the LLDPE-*g*-PS chains added really connect one component of LLDPE/PS blends, LLDPE, through solubilization of chemically identical segments or by isomorphism.

To study the compatibilizing effects of LLDPE-*g*-PS on LLDPE/PS blends, it is not enough only to know the effects of LLDPE-*g*-PS on the morphology of LLDPE. We have to know how the compatibilizers affect the microstructure of the other component, PS, of the LLDPE/PS blends. Figure 4 illustrate the plots of logarithmic intensity of the ^{13}C CPMAS spectrum (peak at 128.0 ppm) of the aromatic group of PS and its blends versus the proton-spin-locking time. Some interesting results can be drawn from Figure 4. First, mixing PS with LLDPE makes the spin relaxation of PS change from exponential [a single $T_{1\rho}(H)$] to biexponential [two $T_{1\rho}(H)$]. One of the $T_{1\rho}(H)$ values of PS in the blends is the same as that of pure PS, and the other $T_{1\rho}(H)$ is much longer than that of pure PS. Naturally, the PS chains in the blends with $T_{1\rho}(H)$ that are the same as that of pure PS can be assigned to the bulk PS domains, and the PS chains with $T_{1\rho}(H)$ much longer than that of pure PS to the domains containing LLDPE and PS (i.e., the interfacial region). Mixing PS with LLDPE (30 wt %) has almost no effect on the $T_{1\rho}(H)$ of the crystalline region of LLDPE (see Fig. 2), but mixing PS with LLDPE (70 wt %) makes the $T_{1\rho}(H)$ of the crystalline region of LLDPE change a lot (see Fig. 1). This means that LLDPE/PS blends are partially miscible, and the miscibility and morphology of LLDPE/PS blends depends on the composition of the blends. Furthermore, the addition of LLDPE-*g*-PS to LLDPE/PS blends makes different changes in the two $T_{1\rho}(H)$ values of PS, depending on the PS grafting yield and molecular structure of LLDPE-*g*-PS. When the PS grafting yield of LLDPE-*g*-PS is smaller, the addition of LLDPE-*g*-PS into LLDPE/PS blends has an obvious effect on the $T_{1\rho}(H)$ of PS chains in the interfacial region, but almost no effect on the $T_{1\rho}(H)$ of PS chains in the bulk PS, suggesting that most of LLDPE-*g*-PS added locate on the interfacial region between the LLDPE and PS domains. With the increase in PS grafting yield of LLDPE-*g*-PS, the addition of LLDPE-*g*-PS into the blends not only influences the $T_{1\rho}(H)$ of PS chains in the interfacial region, but also brings about obvious change in the $T_{1\rho}(H)$ of PS chains in the bulk PS. In consideration of the effect of LLDPE-*g*-PS on the crystallization behavior of LLDPE, we can conclude that LLDPE-*g*-PS really connects two immiscible components, LLDPE

Table IV Effect of LLDPE-*g*-PS Content on T_2 (H) (μs)[a] of LLDPE in LLDPE/PS Blends

LLDPE/PS–GPS27	T_2 (H)	%	T_2 (H)	%
100/0/0	108	38.8	8	61.2
70/30/0	107	36.6	11	63.4
70/30/2	163	32.5	12	68.5
70/30/6	169	27.9	12	72.1
70/30/10	203	28.6	14	71.4

[a] Peak at 30.0 ppm, and estimated error $\leq \pm 5\%$.

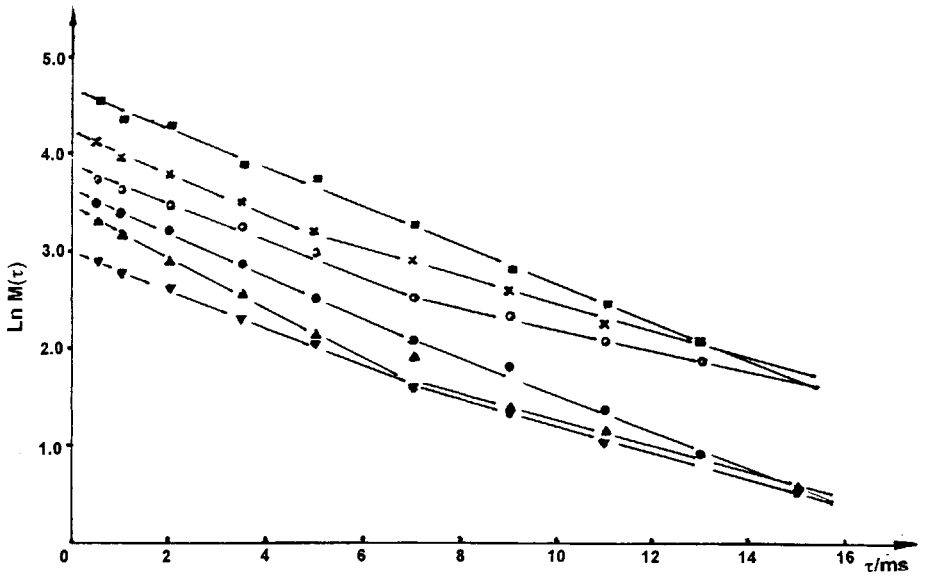

Figure 4 Plots of logarithmic intensity of the ^{13}C CP-MAS spectrum (peak at 128.0 ppm) of PS and its blends versus proton-spin-locking time for (■) PS, (×) LLDPE/PS, (○) LLDPE/PS-GPS4, (●) LLDPE/PS-GPS13, (▲) LLDPE/PS-HGPS17, and (▼) LLDPE/PS-GPS27. The composition of LLDPE/PS-LLDPE-*g*-PS is 28/64/8 by weight.

and PS. Further evidence for LLDPE-*g*-PS connecting the two immiscible components can be inferred from the change in $T_1(C)$ values of the same specimens (see Table V). From Table V it is seen that the $T_1(C)$ values of both LLDPE and PS in the LLDPE/PS (30/70) blends are simultaneously decreased by the addition of LLDPE-*g*-PS. An exception is the blends with compatibilizer synthesized from ethylene and polystyrene–allyl macromonomer due to the higher crystallizability of polyethylene. These results are also in accordance with those from DSC measurements of the same specimens. Finally, the domain sizes of LLDPE in LLDPE/PS blends, measured by proton-spin-diffusion experiments,[17] were obviously reduced by the addition of LLDPE-*g*-PS (see Table VI).

From the aforementioned results, we can draw the following conclusions: (1) LLDPE-*g*-PS is an effective compatibilizer for LLDPE/PS blends. The compatibilizing effect of LLDPE-*g*-PS on LLDPE/PS blends depends on the PS grafting yield and molecular structure of the compatibilizer and also on the composition of LLDPE/PS blends. (2) The possible mechanism of LLDPE-*g*-PS compatibilizing immiscible LLDPE/PS blends is that LLDPE-*g*-PS connects two immiscible components, LLDPE and PS, through solubilization of chemically identical segments in LLDPE-*g*-PS into the amorphous region of LLDPE and PS domains. At the same time, parts of LLDPE chains free branching in LLDPE-*g*-PS connect with crystalline phase of LLDPE by isomorphism, which has an obvious effect on the

Table V Effect of LLDPE-*g*-PS on $T_1(C)$ (s)[a] of LLDPE/PS (30/70) Blends

	PS (128.0 ppm)		LLDPE (32.2 ppm)	
LLDPE-*g*-PS[b]	$T_{1L}(C)$	$T_{1S}(C)$	$T_{1L}(C)$	$T_{1S}(C)$
—	47.6	2.0	74.7	0.5
GPS4	34.4	1.9	31.2	0.4
HGPS17	34.0	0.4	81.4	0.3
GPS27	38.0	1.6	41.6	0.4

[a] Estimated error ≤ ±10%.
[b] The content of LLDPE-*g*-PS in blends is 8% by weight.

Table VI Effect of LLDPE-*g*-PS on Domain Size of LLDPE in LLDPE/PS (30/70) Blends

LLDPE-*g*-PS[a]	LLDPE Domain Size (nm)
—	21.5
GPS4	19.9
GPS13	14.8
HGPS17	15.3
GPS27	17.1

[a] The content of LLDPE-*g*-PS in blends is 8% by weight.

crystallization behavior of LLDPE. As a consequence, the lamellar thickness of LLDPE decreases, and a great quantity of less perfect crystallites forms.

The authors are grateful for the financial support granted by the National Key Projects for Fundamental Research "Macromolecular Condensed State," the State Science and Technology Commission of China, the Laboratory of Magnetic Resonance and Atomic and Molecular Physics, the Wuhan Institute of Physics, and the Chinese Academy of Sciences.

REFERENCES

1. R. Fayt, R. Jerome, and Ph. Teyssie, *J. Polym. Sci. Polym. Phys. Ed.*, **20,** 2209 (1982).
2. D. Heikens, N. Hoen, W. Barentsen, P. Piet, and H. Ladan, *J. Polym. Sci. Polym. Symp.*, **62,** 309 (1978).
3. B. Y. Pietrasanta, M. Taha, and T. Sarraf, *Polym. Bull.*, **14,** 25 (1985).
4. T. Ouhadi, R. Fayt, R. Jerome, and Ph. Teyssie, *J. Appl. Polym. Sci.*, **32,** 5647 (1986).
5. F. Ide and A. Hasegawa, *J. Appl. Polym. Sci.*, **18,** 963 (1974).
6. S. H. Anastasiadis, I. Gancarz, and J. T. Koberstein, *Macromolecules,* **22,** 1449 (1989).
7. S. Wu, *Polym. Eng. Sci.*, **27,** 335 (1987).
8. R. Fayt, R. Jerome, and J. T. Koberstein, *Makromol. Chem.*, **187,** 837 (1986).
9. J. Noolandi and K. M. Hong, *Macromolecules,* **17,** 1531 (1984).
10. S. Datta and D. J. Lohse, *Macromolecules,* **26,** 2064 (1993).
11. H. Feng, C. Ye, J. Tian, Z. Feng, and B. Huang, submitted.
12. S. J. Opella and M. H. Frey, *J. Am. Chem. Soc.*, **101,** 5854 (1979).
13. V. D. Fedotov and H. Schneider, *Structure and Dynamics of Bulk Polymers by NMR-Methods,* Springer-Verlag, Berlin, 1989.
14. D. E. Axelson, L. Mandelkern, R. Popli, and P. Mathieu, *J. Polym. Sci. Polym. Phys. Ed.*, **21,** 2319 (1983).
15. K. J. Packer, I. J. F. Poplett, and M. J. Tayler, *J. Chem. Soc. Faraday Trans.*, **I,** 84, 3851 (1988).
16. B. Wunderlich, *Macromolecular Physics, Vol. 2: Crystal Nucleation, Growth, Annealing,* Academic Press, New York, 1976.
17. P. Tekely, D. Canet, and J. Puech, *J. Mol. Phys.*, **67,** 81 (1989).

Received November 27, 1995
Accepted March 11, 1996